# Search for supersymmetry with R-parity violation at $\sqrt{s}$ = 192 to 208 GeV

R. Barbier, C. Berat, P. Jonsson, V. Poireau

**DELPHI Collaboration**

DELPHI 2001-083 CONF 511
12 June, 2001

# Search for supersymmetry with R-parity violation at $\sqrt{s}$ =192 to 208 GeV

**R. Barbier[1], C. Berat[2], P. Jonsson[1], V. Poireau[3]**
[1]IPN Lyon, [2]ISN Grenoble, [3]CEA/DAPNIA/SPP Saclay.

**Abstract**

Searches for pair production of supersymmetric particles under the assumption of non-conservation of R-parity have been performed using the data collected by the DELPHI experiment at LEP in $e^+e^-$ collisions at centre-of-mass energies from 192 to 208 GeV. No excess of data above Standard Model expectations was observed. The results were used to constrain the MSSM parameter space, and to derive mass limits for SUSY particles.

Contributed Paper for EPS HEP 2001 (Budapest) and LP01 (Rome)

# 1 Introduction

In 2000, the LEP centre-of-mass energy reached 208 GeV, and an integrated luminosity of 224.4 $pb^{-1}$ has been collected by the DELPHI experiment. The data have been analyzed to search for supersymmetric particles in the hypothesis of $R$–parity violation ($\not{R}_p$) [1]. The major consequences of the non conservation of the $R$–parity is the allowed decay of the Lightest Supersymmetric Particle (LSP) in standard fermions and the possibility to produce single supersymmetric particles. The analyses described in this note cover the pair production of supersymmetric particles. The $\not{R}_p$ superpotential [2] contains three trilinear terms, two violating $L$ conservation, and one violating $B$ conservation. We consider here only the $\lambda_{ijk}\mathrm{L}_i\mathrm{L}_j\bar{\mathrm{E}}_k$ (non conservation of $L$) and $\lambda''_{ijk}\bar{\mathrm{U}}_i\bar{\mathrm{D}}_j\bar{\mathrm{D}}_k$ terms (non conservation of $B$) ($i, j, k$ are generation indices), which couple the sleptons to the leptons and the squarks to the quarks respectively.

The Minimal Supersymmetric Standard Model (MSSM) scheme [3] with the assumption that the gaugino masses are unified at the Grand Unified Theories (GUTs) scale is assumed. Relevant parameters for these $\not{R}_p$ searches are then: $\mathrm{M}_1$, $\mathrm{M}_2$, the U(1) and SU(2) gaugino mass at the electroweak scale (with $\mathrm{M}_1 = \frac{5}{3}tan^2\theta_W\mathrm{M}_2$), $\mathrm{m}_0$, the scalar common mass at the GUT scale, $\mu$, the mixing mass term of the Higgs doublets at the electroweak scale and tan$\beta$, the ratio of the vacuum expectation values of the two Higgs doublets. We assume that the running of the $\lambda$ and $\lambda''$ couplings from the GUT scale to the electroweak does not have a significant effect on the "running" of the gaugino and fermion masses.

The LSP is assumed to have a negligible lifetime so that the production and decay vertices coincide. Otherwise the LSP decay vertex is displaced, and the analyses described here become inefficient.

## 1.1 $R$–parity violating decays of supersymmetric particles

### 1.1.1 Direct and Indirect decays

Two types of supersymmetric particle decays are considered. First, the direct decay of sfermion into two standard fermions, or the decay of neutralino (chargino) into a fermion and a virtual sfermion which then decays into two standard fermions. Second, the indirect decay corresponding to the supersymmetric particle cascade decay through $R$–parity conserving vertex to on-shell supersymmetric particles down to the lighter supersymmetric particle which then decays via one $\mathrm{LL}\bar{\mathrm{E}}$ or $\bar{\mathrm{U}}\bar{\mathrm{D}}\bar{\mathrm{D}}$ term.

### 1.1.2 Decays through $\mathrm{LL}\bar{\mathrm{E}}$ terms

The direct decay of a neutralino or a chargino via a dominant $\lambda_{ijk}$ coupling leads to purely leptonic decay signatures, with or without neutrinos ($\ell\ell'\nu$, $\ell\ell'\ell''$, $\ell\nu\nu$). The indirect decay of a heavier neutralino or a chargino adds jets and/or leptons to the leptons produced in the LSP decay.

The sneutrino direct decay gives two charged leptons: via $\lambda_{ijk}$ only the $\tilde{\nu}_i$ and $\tilde{\nu}_j$ are allowed to decay directly into $\ell_j^{\pm}\ell_k^{\mp}$ and $\ell_i^{\pm}\ell_k^{\mp}$ respectively. The charged slepton direct decay gives one neutrino and one charged lepton (the lepton flavor may be different from the slepton one). The supersymmetric partner of the right-handed lepton, $\tilde{\ell}_{kR}$ can only decay directly to in $\nu_{iL}\ell_{jL}$ or $\ell_{iL}\nu_{jL}$.

The indirect decay of a sneutrino (resp. charged slepton) into a neutralino and a neutrino (resp. charged lepton) leads to a purely leptonic final state: two charged leptons and two neutrinos (resp. three charged leptons and a neutrino). With a $LL\bar{E}$ term, only the indirect decay of a squark into a quark and a neutralino (or a chargino) is possible.

When the charged leptons are $\tau$ (for example with $\lambda_{131}$ or $\lambda_{133}$ couplings), additional neutrinos are generated in the $\tau$ decay, producing more missing energy in the decay and leading to a smaller number of charged leptons in the final state.

### 1.1.3 Decays through $\bar{U}\bar{D}\bar{D}$ terms

In case of a dominant $\bar{U}\bar{D}\bar{D}$ term, the neutralino decays via a virtual squark and a quark and subsequently gives a three quarks final state (the squark decays into two quarks via $\bar{U}\bar{D}\bar{D}$ terms). Then for each indirect decay of a chargino, squark or slepton pair, we have at least six quarks in the final state. Therefore the most important feature of these decays are the number of quarks produced which goes up to ten for the indirect decay of two charginos with the hadronic decays of the W bosons. The direct squark decay gives the smallest number of quarks in the final state and were not considered in the squark analysis. In this channel, a large amount of hadronic decay of W and Z boson pair remain as an irreducible background for the four-jet signal. The unique possibility for the sleptons to decay through a $\bar{U}\bar{D}\bar{D}$ term is the indirect decay channel. In this last case, two leptons are produced in the slepton decay in association with six jets.

## 1.2 Pair production of supersymmetric particles

Pair production of supersymmetric particles in MSSM with $\not{R}_p$ is identical to the pair production with $R_p$ conservation, since the trilinear couplings are not present in the production vertex.

The charginos are produced by pairs in the $s$-channel via $\gamma$ or Z exchange, or in the $t$-channel via sneutrino ($\tilde{\nu}_e$) exchange if the charginos have a gaugino component; the neutralinos are produced by pairs via $s$-channel Z exchange provided they have a higgsino component, or via $t$-channel selectron exchange if they have a gaugino component. The $t$-channel contribution is suppressed when the slepton masses (depending on $m_0$) are high enough. When the selectron mass is sufficiently small (less than 100 GeV/$c^2$), the neutralino production can be enhanced, because of the $t$-channel $\tilde{e}$ exchange contribution. On the contrary, if the $\tilde{\nu}_e$ mass is in the same range, the chargino cross-section can decrease due to destructive interference between the $s$- and $t$-channel amplitudes.

Pair production cross-section of sfermions mainly depends on the sfermion masses. The selectron and sneutrino cross-sections are also very sensitive to the chargino and neutralino components (function of $\mu$, $M_2$ and $\tan\beta$) via the $t$–channel exchange. In the case of the third generation, the left-right mixing angle enters in the production cross-section as well. Two cases were considered in the stop analysis to extract mass limits: the first one with no mixing, the second one with the mixing angle corresponding to the squarks decoupling from the Z boson.

# 2 Data samples

Data recorded in 2000 by the DELPHI detector (described in details in [7]) at centre-of-mass energies up to $\sqrt{s} = 208$ GeV, corresponding to an integrated luminosity of about 160 pb$^{-1}$ among the total of 224 pb$^{-1}$, have been analysed. The events collected when one sector of the Time Projection Chamber [7] did not work were not taking into account.

To evaluate background contaminations, different contributions coming from the Standard Model processes were considered. The Standard Model events were produced by the following generators:

- $\gamma\gamma$ events: `BDK` [8] for $\gamma\gamma \rightarrow \ell^+\ell^-$ processes, and `TWOGAM` [9] for $\gamma\gamma \rightarrow$ hadron processes.
- two-fermion processes: `BHWIDE` [10] for Bhabhas, `KORALZ` [11] for $e^+e^- \rightarrow \mu^+\mu^-(\gamma)$ and for $e^+e^- \rightarrow \tau^+\tau^-(\gamma)$ and `PYTHIA` [12] for $e^+e^- \rightarrow q\bar{q}(\gamma)$ events.
- four-fermion processes: The four fermion background was generated with `EXCALIBUR` [13] in most of the phase space but also `GRC4F` [14] was used to complete the `EXCALIBUR` samples in the case of very forward electrons.

Signal events were generated with the `SUSYGEN` program [15] followed by the full DELPHI simulation and reconstruction program (`DELSIM` [7]).

# 3 Description of the analyses

For all the analyses presented in this section, it was assumed that only one $\lambda_{ijk}$ or $\lambda''_{ijk}$ is dominant at a time, and its upper bound, derived from indirect searches of $R$–parity violating effects [4]–[6], has been taken into account for the generation of the signals.

The analyses presented in what follows are updates of the 1999 data analyses, which have been extensively described in [17].

## 3.1 Search for pair production in case of $LL\bar{E}$ terms

Two types of analyses have been performed:

- the first one assumes that $\lambda_{122}$ is dominant (i.e the charged leptons coming from $\not{R}_p$ decay are muons and electrons). This is the most efficient and selective case since the selection criteria are based on e and $\mu$ identification;
- the second search assumes that $\lambda_{133}$ is dominant, meaning that the leptons from $\not{R}_p$ decay are mainly taus and electrons. This is the case with the lowest efficiency and the lowest rejection power due to the presence of several taus in the final state.

Any of the possible topologies should be covered by one of the two analysis types, to be sure that any type of $\not{R}_p$via LLE coupling signal could be discovered. Two different $\lambda_{ijk}$ can lead to the same final state, and therefore the same efficiency ranges. This allows to apply the first type of analysis to signals produced via $\lambda_{2j2}$. In most cases, the analyses of the second type are applied to signals generated with other $\lambda_{ijk}$, and the efficiencies are either of the same order or higher than for $\lambda_{133}$ signals.

The applied sequential selections were based on the criteria already presented in [16, 17], using mainly missing quantities, lepton identification (based on standard DELPHI algorithms) and kinematic properties, and jet characteristics. Jets can be produced in indirect decays of sparticles, and thin jets in the $\tau$ decays. The jets were reconstructed

with the DURHAM [18] algorithm. In order to cover the different topologies, the jet number was not fixed, and the jet charged multiplicity could be low (thin jets with one charged particle for instance).

Since no signal has been observed, the results of the $\lambda_{133}$ analysis are used to derive the most conservative limits, and then only informations on the $\lambda_{133}$ analyses are given in the present note.

### 3.1.1 LL$\bar{\text{E}}$ term: charginos and neutralinos searches

The $\widetilde{\chi}_i^0$ and $\widetilde{\chi}_k^{\pm}$ pair production were considered for different values of tan$\beta$ (from 0.7 to 30), $m_0$ (between 90 GeV/$c^2$ and 500 GeV/$c^2$), $\mu$ (between –200 GeV/$c^2$ and 200 GeV/$c^2$) and $M_2$ (between 5 and 400 GeV/$c^2$).

In the search for neutralino and chargino pair production in case of a dominant $\lambda_{133}$ coupling, the preselection requirements described in [17] were used. After this preselection, 1230 real data remained for $1146 \pm 5$ events expected from Standard Model processes; the agreement between the number of observed and expected events at the preselection level was satisfactory. At the end of the selection, it remains 9 events for 8.0±0.4 expected.

The selection efficiencies were computed from simulated samples for different points of the MSSM parameters space. A global event selection efficiency has been determined at each point, and was in the range 13–38% in case of a dominant $\lambda_{133}$ coupling.

### 3.1.2 LL$\bar{\text{E}}$ term: sleptons searches

In case of sneutrino direct decay (Br($\tilde{\nu} \rightarrow \ \ell^+\ell^-$) = 100%), the processes $\widetilde{\nu}_{\text{e}}\widetilde{\bar{\nu}}_{\text{e}} \rightarrow 4\mu$ ($\lambda_{122}$), $\widetilde{\nu}_{\text{e}}\widetilde{\bar{\nu}}_{\text{e}} \rightarrow 4\tau$ ($\lambda_{133}$), $\widetilde{\nu}_{\mu}\widetilde{\bar{\nu}}_{\mu} \rightarrow 4\tau$ ($\lambda_{233}$) and $\widetilde{\nu}_{\tau}\widetilde{\bar{\nu}}_{\tau} \rightarrow$ 2e2$\tau$ ($\lambda_{133}$) have been generated for different values of sneutrino mass up to 100 GeV/$c^2$, with tan$\beta$ and $\mu$ fixed at 1.5 and –150 GeV/$c^2$ respectively. In order to be sure that all final states were covered, signals obtained for other $\lambda_{ijk}$ couplings and for sneutrino mass around 95 GeV/$c^2$ were also generated. Events with sneutrino (slepton) indirect decay (Br($\tilde{\nu}$ ($\tilde{\ell}$) $\rightarrow \widetilde{\chi}_1^0\nu$ ($\ell$)) = 100%) were also simulated with $\lambda_{122}$ and $\lambda_{133}$ couplings, for different $\tilde{\nu}$ ($\tilde{\ell}$) and $\widetilde{\chi}_1^0$ masses, in order to cover several ranges of mass difference between sneutrinos (sleptons) and neutralinos. Furthermore, in case of slepton indirect decays, selectron, smuon and stau pair productions have been simulated, since the efficiencies depend also on the slepton flavor.

The results of the analyses applied to cover final states produced when a $\lambda_{122}$ coupling is dominant are given in table 1. They concern the direct decay of $\widetilde{\nu}_{\text{e}}$ or $\widetilde{\nu}_{\mu}$ pairs, the indirect decay of sneutrino pairs, and the indirect decay of smuon pairs. No excess of candidate events was found in the 2000 data.

When $\lambda_{133}$ coupling is dominant, mainly taus are produced in the final states. Then there are always neutrinos coming from the $\tau$ decay, eventually with additional neutrinos which could be produced at the $\not{R}_p$ vertex.

The analyses were designed to cover two main topologies:

- the 2$\tau$2e final states (missing energy coming from the tau decay only), from the direct decay of $\widetilde{\nu}_{\tau}$ pairs;

- the 4 or 6 leptons and missing energy final states, with at least 2 taus, from the indirect decay of any sneutrino pair; and from the indirect decay of a slepton pair.

The same preselection procedure, as described in [17], can be settled for the two analyses. After it, 822 events remain in the data, for 814±4 expected from the background sources.

One selection is designed to search for leptonic final states with a large amount of missing energy. At the end, 5 events remained in the data compared to $3.3 \pm 0.3$ expected from the Standard Model processes. The background was mainly composed of four-fermion events, in particular from the W pair production. The second analysis is designed to select events with less missing energy, and at the end, 2 candidates were obtained for $2.1 \pm 0.2$ expected.

In case of direct decay of $\widetilde{\nu}_e$ pair in $4\tau$, the first analysis was applied, and the efficiency was between 26% and 36%, depending on the sneutrino mass. It laid in the same range for the sneutrino indirect decay, depending also on the neutralino mass, but not on the sneutrino flavour. The efficiencies were higher for final states obtained in indirect decay of slepton pairs, due to the presence of two additional leptons. They ranged from 33% to 42% for stau pairs, and were 5% to 8% higher for selector and smuon pairs (in this case indeed the two additional leptons are either electrons or muons). The second analysis was applied to cover the direct decay via $\lambda_{133}$ of $\widetilde{\nu}_\tau$ pair; the efficiencies varied with the $\tilde{\nu}_\tau$ mass and ranged from 44% to 51%. The results of these analyses are summarized in Table 1.

### 3.1.3 $LL\bar{E}$ term: stop searches

In the case of stop pair production, each of the stops decays into a charm quark and a neutralino, and, with the subsequent $\not{R}_p$ decay of the neutralino into leptons, the final state is composed of two jets + four charged leptons + missing energy. Signals corresponding to these stop pair decays were generated for several sets of stop and neutralino masses.

The analysis performed in the case of a dominant $\lambda_{133}$ coupling leads to the most conservative limit on the stop mass. The same preselection and selection criteria as described in [17] were used to select the final states of the stop pair indirect decay. The preselection was efficient to suppress the background coming from Bhabha scattering and two-photon processes, and to remove a large part of the $f\bar{f}(\gamma)$ contribution. After this preselection stage, 786 events were selected for $803 \pm 4$ expected from the background sources. 11 events remained after the selection procedure, with $11.6 \pm 0.3$ expected from background contribution. The main background contribution comes from the $W^+W^-$ production.

The selection efficiencies varied with the stop mass and with the mass difference between the stop and the lightest neutralino. They laid around 30%, except in two cases: for low neutralino masses, the efficiencies were around 10–17%, and in the degenerate case (i.e the mass lower than 5 GeV/$c^2$), the efficiency decreased and went down to almost 0 for $m_{\tilde{t}} - m_{\tilde{\chi}^0} = 2$ GeV/$c^2$. This analysis was not optimized for topologies produced when the mass difference is below 5 GeV/$c^2$, therefore it was not sensitive to the very degenerate case.

## 3.2 Search for pair production in case of $\bar{\mathrm{U}}\bar{\mathrm{D}}\bar{\mathrm{D}}$ terms

The present studies covered the search for $\widetilde{\chi}_1^0$, $\widetilde{\chi}_1^+$, $\widetilde{q}$ and $\widetilde{\ell}$ pair production previously studied in 1998 and 1999 [17]. The analysis of the different decay channels can be organized on the basis of the number of hadronic jets in the final state and on the mass difference between the studied sparticle and the LSP.

**Clustering algorithm**
For each multi-jet analysis, the clustering of hadronic jets was performed by the *ckern* package [19] based on the Cambridge clustering algorithm [20]. For each event, *ckern* provides all possible configurations between 2 and 10 jets. The values of the variables $\mathrm{y}_{n\ n-1}$ (for $n$ between 2 and 10), were a powerful tool to identify the topologies of the multi-jet signals.

**Signal selection with neural networks**
A neural network method was applied in order to distinguish signals from Standard Model background events for all multi-jets analysis except for the 6 jets + 2 muons analysis which have been performed with a sequential method (the very good muon identification of the detector gave sufficient signal discrimination from hadronic background). The SNNS package [21] and MLPFit package [22] were used for the training and the validation of the neural networks. The training was done on samples of simulated background and signal. The exact configuration and input variables of each neural network depended on the search channel. Each neural network provided a discriminant variable which was used to select the final number of candidate events for each analysis.

### 3.2.1 $\bar{\mathrm{U}}\bar{\mathrm{D}}\bar{\mathrm{D}}$ term: chargino and neutralino searches

After the preselection step described in [17], the main background events were the four-fermion events and the $\mathrm{f\bar{f}}\gamma$ QCD events with hard gluon radiation. We observed 3844 events in the data for 3869 expected events from background processes (for centre-of-mass energies between 202 and 208 GeV). The preselection efficiencies were varying from 73% to 100% for the direct decay signals, and from 60% to 98% for the indirect decay signals, depending on the simulated masses.

It was shown that the modelisation of the gluon emission is unable to correctly describe the high number of jet region. To take into account this imperfect description, corrections [17] were applied on the values of $\mathrm{y}_{n\ n-1}$ (for $n$ between 6 and 10, i.e. for variables characteristic of the high number of jets).

The direct and indirect decay analyses were based on a neural network method for the optimization of the background and signal discrimination. The neural network package used was MLPFit. The discriminating variables were used as inputs of the one hidden layer neural network. The signal output node was used for the signal selection. Each neural network (one per mass window, as explained in the next sections) was trained on 206 GeV simulated background and signal samples. The training was done on the whole range of simulated signal masses belonging to the window analysis.

**Direct decay of $\widetilde{\chi}_1^0\widetilde{\chi}_1^0$ or $\widetilde{\chi}_1^+\widetilde{\chi}_1^-$ into 6 jets**

Events with low chargino or neutralino masses have a large boost and look like 2-jet events. On the contrary, heavy chargino or neutralino events are almost spherical with 6 well separated jets. Therefore, we distinguished 3 mass windows to increase the sensitivity of each signal configuration:

- window N1; low masses: $10 \leq m_{\tilde{\chi}} \leq 45$ GeV/$c^2$,
- window N2; medium masses: $45 < m_{\tilde{\chi}} \leq 75$ GeV/$c^2$,
- window N3; high masses: $m_{\tilde{\chi}} > 75$ GeV/$c^2$.

A mass reconstruction was performed using a method depending on the mass window. For the N1 window analysis, the events were forced into 2 jets and the average of the masses was computed. For the two last windows, the events were forced into 6 jets and criteria on di-jet angles were applied to choose the best 3-jet combination.

Three neural networks were used (one per mass window) with the following variables as inputs:

- thrust,
- dist$_{WW}$= $\sqrt{\frac{(M_1-M_2)^2}{\sigma_-^2} + \frac{(M_1+M_2-2M_W)^2}{\sigma_+^2}}$ with $M_1$ and $M_2$ were the di-jet masses of the jet combination which minimized this variable (after forcing the event into 4 jets); we took $M_W = 80.4$ GeV/$c^2$ for the $W$ mass, $\sigma_- = 9.5$ GeV/$c^2$ and $\sigma_+ = 4.8$ GeV/$c^2$ for the mass resolutions on the difference and the sum of the reconstructed di-jet masses respectively; this variable is peaked to 0 for WW events, allowing a good discrimination against this background,
- energy of the least energetic jet $\times$ minimum di-jet angle in 4 and 5 jet configurations,
- reconstructed mass,
- energy difference between the 2 objects after the mass reconstruction,
- -log(y$_{n\ n-1}$) with $n$=3 to 10 (for $n$=6 to 10, the corrected variables were used).

As an example, Figure 1a shows the number of expected events from the Standard Model and the number of observed events as a function of the average signal efficiency for the N3 mass window. No excess of events was seen in the data with respect to the Standard Model expectations, therefore we optimized the cut on the neural network by minimizing the expected limit on the excluded cross-section. In order to obtain signal efficiencies, the full detector simulation was performed on neutralino pair production with a 10 GeV/$c^2$ step grid in the neutralino mass (10 to 103 GeV/$c^2$). The efficiencies were typically around 30-60% at the values of the optimized neural network outputs, depending on the simulated masses. The statistical errors on the efficiency were typically 1.5%, which was comparable to the systematic ones. The expected and observed numbers of events are reported in Table 2 for each mass window. The errors given in the Table are a combination of the statistic and the systematic errors. No excess was observed for any working point.

**Indirect decay of $\widetilde{\chi}_1^+\ \widetilde{\chi}_1^-$**

The indirect decay of charginos gives events with 6 to 10 jets, with possibly charged leptons and neutrinos, depending on the decay of the two off-shell W bosons. To take into account the effect of the mass difference $\Delta M$ between chargino and neutralino on the topology of the event, we divided the indirect decay analysis into 2 windows:

- window C1; low chargino neutralino mass difference: $\Delta M \leq 10$ GeV/$c^2$,
- window C2; high chargino neutralino mass difference: $\Delta M > 10$ GeV/$c^2$.

Two neural networks were trained with discriminating topological variables as input nodes. These variables were identical to the direct decay analysis, except for those concerning the mass reconstruction.

The expected number of events from the Standard Model and the number of selected data events as a function of the average signal efficiency are shown for the C2 window (Figure 1b). The optimal neural network outputs have been derived with the same procedure as for the direct decay analysis. No significant excess was found in the number of observed events. The signal efficiencies were obtained by simulating chargino pair production by step of 10 GeV/$c^2$ on the masses in a 2-dimensional grid (from 10 to 100 GeV/$c^2$ for $\widetilde{\chi}_1^0$ and from 50 GeV/$c^2$ to 103 GeV/$c^2$ for $\widetilde{\chi}_1^+$). These efficiencies were between 10% and 70%, the statistical errors around 1.5% and the systematic errors around 1%. Table 3 summarizes the comparison between data and background expectations. The given errors are the quadratic sum of the statistic and the systematic errors.

### 3.2.2 $\bar{\mathrm{U}}\bar{\mathrm{D}}\bar{\mathrm{D}}$ term: smuons and selectrons searches

Searches for selectrons and smuons were performed in the case of indirect decays (the only possible decay with a $\bar{\mathrm{U}}\bar{\mathrm{D}}\bar{\mathrm{D}}$ term). Due to the existing limit on the chargino mass these analyses were based on the indirect decay of the slepton i.e. the lepton-neutralino channel.

Slepton signals were simulated with SUSYGEN [15] at different slepton masses by a step of 10 GeV/$c^2$. The points were simulated from 45 to 95 GeV/$c^2$ for sleptons mass and from 25 to 90 GeV/$c^2$ for the $\widetilde{\chi}_1^0$ mass up to $\Delta\mathrm{M} = \mathrm{m}_{\tilde{\ell}} - \mathrm{m}_{\tilde{\chi}^0} = 5$ GeV/$c^2$.

These two channels have final states with a large hadronic activity and this is true independently on the mass difference between the slepton and the neutralino. The momentum of the lepton coming from the indirect decay of the slepton have been used for the signal selection. Therefore electron and muon identifications were used in these 2-leptons and multi-jets analyses. After the hadronic preselection step, we observed 2833 events in the data for 2835 expected events from background processes.

Two analysis windows, $\Delta M \leq 10$ GeV/$c^2$ and $\Delta M > 10$ GeV/$c^2$, with different signal selection optimisation have been used, to take into account the mass difference between the slepton and the neutralino. A logical .OR. analysis on the two window mass selections has been used to obtain the final numbers of data and expected background events from SM processes.

### 2e + 6 jets channel: $\bar{\mathrm{U}}\bar{\mathrm{D}}\bar{\mathrm{D}}$ term: selectron

The neural network optimized for the analysis of the 99 data [17] have been used for this analysis. Three output nodes had been defined: one for the signal, one for the $q\bar{q}(\gamma)$ background and one for the 4-fermions.

The final selection of candidate events was based on the signal output value of the neural networks (0.94 for $\Delta M \leq 10$ GeV/$c^2$ and 0.95 for $\Delta M > 10$ GeV/$c^2$) minimizing the expected excluded cross-section. The two signal outputs values are shown in Figure 2. After an logical .OR. analysis on the two windows, no excess of data over Standard Model expectations was observed for the selectrons analysis. The numbers of events observed and expected from backgrounds are shown in Table 4.

The signal efficiency was evaluated at each of the 33 simulated points and interpolated

in the regions between. Efficiencies for the signal were in the range from 5-40%, for small mass differences, and increased up to 80% for $\Delta M > 10$ GeV/$c^2$ mass window. The statistical errors on signal efficiencies were typically 2%.

**$2\mu$ + 6 jets channel: $\bar{\mathrm{U}}\bar{\mathrm{D}}\bar{\mathrm{D}}$ term: smuons**

A sequential analysis on the whole mass plane described in [17], based mostly on the momenta of the two muons and on the $y_{n\ n-1}$ distribution shown in figure 3, had been performed instead of using a neural network optimisation of the signal selection. The better muon identification efficiency compare with the electron one gave sufficient background rejection with a good signal selection efficiency.

No excess of data over Standard Model backgrounds was observed for this analysis. The numbers of events observed and expected from backgrounds are shown in Table 4.

### 3.2.3 $\bar{\mathrm{U}}\bar{\mathrm{D}}\bar{\mathrm{D}}$ term: squarks searches

Searches for pair produced stops were performed in the case of indirect decays through a single dominant $\bar{\mathrm{U}}\bar{\mathrm{D}}\bar{\mathrm{D}}$ term. The eight quark event topology depends strongly on the difference in mass between the squark and the $\widetilde{\chi}_1^0$.

SUSY signals were simulated at different squark masses in the range 50–90 GeV/$c^2$ with $\widetilde{\chi}_1^0$ masses between 30–85 GeV/$c^2$. The simulated decay used for the efficiency evaluation was $\widetilde{b} \rightarrow b\ \widetilde{\chi}_1^0$ with $\widetilde{\chi}_1^0$ going to three light quarks.

The final selection of candidate events was based on the output values of two neural networks (SNNS package). The stop analysis was divided into two $\Delta\mathrm{M} = \mathrm{m}_{\tilde{\mathrm{t}}} - \mathrm{m}_{\tilde{\chi}^0}$ windows ($\Delta\mathrm{M} < 10$ GeV/$c^2$ and $\Delta\mathrm{M} > 10$ GeV/$c^2$) with different neural networks. The following quantities were used as input for the neural networks:

- the total number of charged particles,
- the oblateness of the event,
- -log($y_{n\ n-1}$) with $n = 3$ to 10,
- the $\chi^2_{M_W}$ of the constraint fit for the W mass reconstruction in 4 jets,
- the variables $\alpha_{min} \times E_{min}$ in the 4 and 5 jet topologies,
- the variable $\beta_{min} \times E_{max}/E_{min}$ in the 4 jet topology.

No excess of data over Standard Model expectations was observed for the stop analysis, therefore a working point optimization on the neural network output was performed, minimizing the expected excluded cross-section as a function of the average signal efficiency of the mass window. The numbers of events observed and expected from SM processes are shown in Table 5.

The signal efficiency was evaluated at each of the 30 uniformly distributed simulated points in the plane of squark and neutralino masses and interpolated in the regions between. Efficiencies for the signal after the final selection were in the range from 10-20%, for small or large mass differences between squark and neutralino, up to around 50% for medium mass differences. The statistical errors on the signal efficiencies were typically below 2%.

# 4 Interpretation of the results in the MSSM framework

The results of the searches presented in this paper were in agreement with the Standard Model expectation. They were combined to extend the previously excluded part of the MSSM parameter space and to update limits obtained with similar analyses performed on 1999 data [17].

## 4.1 Results from gaugino pair production study with $\mathrm{L}\mathrm{L}\bar{\mathrm{E}}$ terms

The number of expected events corresponding to gauginos pair production in each point of the explored MSSM parameter space was obtained by:

$$\mathrm{N_{exp}} = \epsilon_g \times \{\sum_{E_{cm}=192}^{E_{cm}=208} \mathcal{L}_{E_{cm}} \times \{\sum_{i,j=1}^{4} \sigma(\mathrm{e^+e^-} \rightarrow \widetilde{\chi}_i^0 \widetilde{\chi}_j^0) + \sum_{k,l=1}^{2} \sigma(\mathrm{e^+e^-} \rightarrow \widetilde{\chi}_k^+ \widetilde{\chi}_l^-)\}\}$$

where $\mathcal{L}_{E_{cm}}$ is the integrated luminosity collected at the centre-of-mass energy $E_{cm}$, and $\epsilon_g$ is the global efficiency determined as explained in section 3.1.1. This number has been compared to the number of signal events, $\mathrm{N_{95}}$, expected at a confidence level (C.L.) of 95% in presence of background, determined following the Bayesian method [24]. All points which satisfied $\mathrm{N_{exp}} > \mathrm{N_{95}}$ were excluded at 95% C.L. The analysis performed considering the $\lambda_{133}$ coupling as the dominant one provided the most conservative constrains on the MSSM parameter values. The corresponding excluded area in $\mu$, $\mathrm{M_2}$ planes obtained with the present searches are shown in Figure 4, for $\mathrm{m_0}$ = 90, 500 GeV/$c^2$ and tan$\beta$ =1.5, 30.

For each tan$\beta$, the highest value of neutralino mass which can be excluded has been determined in the $\mu$, $\mathrm{M_2}$ plane (–200 GeV/$c^2 \leq \mu \leq$ 200 GeV/$c^2$, 5 $< \mathrm{M_2} \leq$ 400 GeV/$c^2$) for several $\mathrm{m_0}$ values from 90 to 500 GeV/$c^2$; the most conservative mass limit was obtained for high $\mathrm{m_0}$ values. The corresponding limit on neutralino mass as a function of tan$\beta$ is shown in Figure 5.

The same procedure has been applied to determine the most conservative lower limit on the chargino mass. The result is less dependent on tan$\beta$, allowing to almost reach the kinematic limit for any value of tan$\beta$.

The lower limit obtained on the neutralino mass is 40 GeV/$c^2$, and the one on the chargino mass is 103 GeV/$c^2$.

## 4.2 Results from gaugino pair production study with $\bar{\mathrm{U}}\bar{\mathrm{D}}\bar{\mathrm{D}}$ terms

The number of signal events ($\mathrm{N_{95}}$) expected at 95% confidence level with presence of background was calculated from data and SM event numbers obtained for all energies [25]. The signal efficiency for any value of $\widetilde{\chi}_1^0$ and $\widetilde{\chi}^{\pm}$ masses was interpolated using an efficiency grid determined with signal samples produced with the full DELPHI detector simulation. For typical values of tan$\beta$ and $\mathrm{m_0}$, the ($\mu$,$M_2$) point was excluded at 95% confidence level if the expected number of signal taking into account the selection efficiency at this point was greater than the $\mathrm{N_{95}}$.

Adding the direct decay analysis and the indirect decay analysis results, an exclusion contour in the ($\mu$, $\mathrm{M_2}$) plane at 95% confidence level was derived for different values of $\mathrm{m_0}$ (90 and 300 GeV/$c^2$) and tan$\beta$ (1.5 and 30). Statistic and systematic errors were taken into account for this exclusion domain. The results obtained for the energies from

192 to 208 GeV were combined to obtain the exclusion contours shown in Figure 6. In the exclusion plots, the main contribution comes from the study of the chargino indirect decays due to the high cross-section. The direct decay analysis becomes crucial in the exclusion plot for low tan$\beta$ value, low $m_0$ values and negative $\mu$ values. 95 % C.L. lower limits on the mass of the lightest neutralino and chargino are obtained from the scan on tan$\beta$ value from 0.5 to 30. The lower limit on the neutralino mass of 38 GeV/$c^2$ is obtained for tan$\beta$ equal to 1 and $m_0$ = 500 GeV/$c^2$ (Figure 7). The chargino is mainly excluded up to the kinematic limit at 102.5 GeV/$c^2$. Note that these results are valid for a neutralino mass greater than 10 GeV/$c^2$.

## 4.3 Results from slepton pair production study with $LL\bar{E}$ terms

The results of the searches for $4\mu$, $2e2\mu$ and $2e2\tau$ final states were combined with those obtained on 1999 data to derive the excluded sneutrino mass values at a confidence level of 95%, taking into account the efficiencies determined when varying the sneutrino mass, and the integrated luminosities at the different centre-of-mass energies. The results from the $4\tau$ search were used to derive limits on $\widetilde{\nu}_e$ ($\lambda_{133}$) and on $\widetilde{\nu}_\mu$ ($\lambda_{233}$), those from the $2e2\tau$ to derive limits on $\widetilde{\nu}_\tau$ ($\lambda_{133}$).

For the $\tilde{\nu}$ indirect decay in $\nu\widetilde{\chi}_1^0$ with the $\not{R}_p$ decay of the neutralino via $\lambda_{133}$, the efficiencies depend on the sneutrino and neutralino masses. The results of the $\lambda_{133}$ analyses on 1999 and 2000 were combined to exclude an area in the $m_{\tilde{\chi}^0}$ versus $m_{\tilde{\nu}}$ plane, as shown in Figure 8. This exclusion area is also valid for the other couplings.

The same procedure has been followed for the charged slepton indirect decays, and the area excluded in the $m_{\tilde{\chi}^0}$ versus $m_{\tilde{\ell}_R}$ plane is plotted in Figure 8. The region where $m_{\tilde{\ell}_R}$ - $m_{\tilde{\chi}^0}$ is less than 2–3 GeV/$c^2$ is not covered by the present analysis, since then the direct decay becomes the dominant mode, leading to two leptons and missing energy signature. Since the selection of indirect decay of a $\widetilde{\tau}_R$ pair into two taus and two neutralinos is less efficient than for the $\widetilde{e_R}$ or $\widetilde{\mu_R}$ pair, the exclusion plot derived from the analysis results of the $\widetilde{\tau}_R$ indirect decay with a dominant $\lambda_{133}$ is valid for any slepton flavour in the hypothesis of a branching fraction $\tilde{\ell}_R \to \ell\widetilde{\chi}_1^0$ equal to 1.

## 4.4 Results from slepton pair production study with $\bar{U}\bar{D}\bar{D}$ terms

From the search of selectron and smuon pair production in case of a dominant $\bar{U}\bar{D}\bar{D}$ term, exclusion domains combining 1999 and 2000 data, have been computed at 95 % of confidence level with the method developped in [26] (Figure 9). The MSSM values taken for these exclusion plots were tan $\beta$ = 1.5 and $\mu$ = –200 GeV/$c^2$. The $M_2$ value was fixed for each neutralino mass. Due to the existing mass limit on the chargino mass we used 100 % of BR for the decay of the slepton into neutralino lepton. The lower limit on the right-handed selectron was 92 GeV/$c^2$ for $m_{\tilde{e}_R} - m_{\tilde{\chi}^0} > 5$ GeV/$c^2$. The lower limit obtained for the right-handed smuon was 85 GeV/$c^2$ for the same $m_{\tilde{\mu}_R} - m_{\tilde{\chi}^0} > 5$..

## 4.5 Results from stop pair production study with $LL\bar{E}$ terms

The results of the search for the stop indirect decay to charm and neutralino, with the subsequent $\not{R}_p$ decay of the neutralino in leptons, were combined with those obtained on 1999 data: a lower limit on the stop pair production cross-section was derived as a

function of the stop and neutralino masses. Using the efficiencies determined for various values of the neutralino mass, and considering the lowest MSSM cross-section for the stop pair production in case of a maximal decoupling to the Z boson (mixing angle = 56°), the exclusion limit was derived in the $m_{\tilde{t}}$, $m_{\tilde{\chi}^0_1}$ plane, as shown in Figure 10. Taking into account that the neutralino mass is above 40 GeV/$c^2$ the lower bound on stop mass is 87 GeV/$c^2$ at 95% C.L., valid for a mass difference between the stop and the neutralino greater than 5 GeV/$c^2$.

### 4.6 Results from stop pair production study with $\bar{\mathrm{U}}\bar{\mathrm{D}}\bar{\mathrm{D}}$ terms

The exclusion procedure used for the gaugino exclusion was applied to the stop analysis. The resulting exclusion contours for stop can be seen in Figure 11. A 100% branching ratio of indirect decays in the neutralino channel was assumed. The mixing angle $\Phi_{mix} = 56°$ corresponds to a decoupling of the stop from the Z boson.

By combining the exclusion contours from the stop search with the constraint on the neutralino mass from the gaugino searches, lower bounds on the squark masses with $\Delta M = m_{\tilde{q}} - m_{\tilde{\chi}^0} > 5$ GeV/$c^2$ were achieved. The lower mass limit on the stop is 87 GeV/$c^2$ in the case of no mixing, and 75 GeV/$c^2$ in the case of maximal Z-decoupling.

## 5 Summary

A great number of searches for supersymmetry with $R$–parity violation have been performed on the data recorded in 2000 by DELPHI. Current mass limits for pair produced sparticles are summarized in Table 6 for different $\not{R}_p$ couplings and decay modes.


### Acknowledgements

The financial support of STINT, The Swedish Foundation for International Cooperation in Research and Higher Education, and NFR, The Swedish Natural Science Research Council, is highly appreciated.

| Coupling | final state | data | MC S.M. | $\varepsilon$ ranges (%) |
|---|---|---|---|---|
| $\lambda_{122}$ | $\mathbf{4\mu}$ / $\mathbf{2\mu 2e}$ | 0 | 0.45±0.07 | 40–50 |
| | $\mathbf{2\mu 2\ell + E_{miss}}$ | 2 | 1.1±0.1 | 50–60 |
| | $\mathbf{4\mu 2\ell + E_{miss}}$ | 0 | 0.9±0.1 | 65–75 |
| $\lambda_{133}$ | $\mathbf{4\tau}$<br>$\mathbf{2\tau 2\ell + E_{miss}}$<br>$\mathbf{2\tau 4\ell + E_{miss}}$ | 5 | 3.3 ±0.3 | 26–36<br>26–37<br>33–42 |
| | $\mathbf{2e2\tau}$ | 2 | 2.1±0.2 | 44–51 |

Table 1: LL$\bar{\text{E}}$: Results of the analyses performed to search for pair production of sleptons.

| Window | Data | Backgrounds | ff$\gamma$ | Four-fermion |
|---|---|---|---|---|
| N1 | 121 | 119.3 $\pm$ 8.7 | 91.7 | 27.6 |
| N2 | 167 | 164.7 $\pm$ 5.7 | 49.0 | 115.7 |
| N3 | 82 | 91.7 $\pm$ 2.3 | 10.0 | 81.7 |

Table 2: $\bar{\mathrm{U}}\bar{\mathrm{D}}\bar{\mathrm{D}}$: Number of selected events in data and corresponding expectations from Standard Model processes for the three mass windows of the **direct decay 6 jets** analysis.

| Window | Data | Backgrounds | ff$\gamma$ | Four-fermion |
|---|---|---|---|---|
| C1 | 156 | 171.7 $\pm$ 5.2 | 32.6 | 139.1 |
| C2 | 20 | 23.5 $\pm$ 1.0 | 3.4 | 20.1 |

Table 3: $\bar{\mathrm{U}}\bar{\mathrm{D}}\bar{\mathrm{D}}$: Number of selected events in data and corresponding expectations from Standard Model processes for the two windows of the chargino **indirect decay 10 jets** analysis.

| Analysis | Data | Backgrounds | ff$\gamma$ | Four-fermion |
|---|---|---|---|---|
| **selectron** | 10 | 14.1 $\pm$ 0.5 | 1.5 $\pm$ 0.2 | 12.6 $\pm$ 0.2 |
| **smuon** | 5 | 3.1 $\pm$ 0.2 | 0.4 $\pm$ 0.1 | 3.49 $\pm$ 0.1 |

Table 4: $\bar{\mathrm{U}}\bar{\mathrm{D}}\bar{\mathrm{D}}$: Number of selected events in 2000 data and corresponding expectations from Standard Model processes for the two **6-jet +2 leptons** analyses.

| Window | Data | Backgrounds | ff$\gamma$ | Four-fermion |
|---|---|---|---|---|
| stop $\Delta$M $<$ 10 GeV | 47 | 52.2$\pm$0.8 | 6.6 | 45.6 |
| stop $\Delta M >$ 10 GeV | 36 | 35.3$\pm$0.7 | 4.4 | 30.9 |

Table 5: $\bar{\mathrm{U}}\bar{\mathrm{D}}\bar{\mathrm{D}}$: Number of selected events in the 2000 data and corresponding expectations from Standard Model processes for the two mass windows of the **8-jet stop** analysis.

| Pair production of | LL$\bar{\text{E}}$ analyses | | $\bar{\text{U}}\bar{\text{D}}\bar{\text{D}}$ analyses | |
|---|---|---|---|---|
| | direct | indirect | direct | indirect |
| $\widetilde{\chi}_1^0$ | **40**[1] | **40**[1] | **38**[1] | **38**[1] |
| $\widetilde{\chi}_1^+$ | **103**[1] | **103**[1] | **102.5**[1] | **102.5**[1] |
| $\widetilde{e}_R$ | **-** | **87**[2] | × | **92**[3] |
| $\widetilde{\mu}_R$ | **-** | **87**[2] | × | **85**[3] |
| $\widetilde{\tau}_R$ | **-** | **87**[2] | × | **-** |
| $\widetilde{\nu}_e$ | **94** | **-** | × | **-** |
| $\widetilde{\nu}_\mu$ | **95** | **87**[4] | × | **-** |
| $\widetilde{\nu}_\tau$ | **95** | **87**[4] | × | **-** |
| $\widetilde{t}_L$ | × | **-** | **-** | **87**[3] |
| $\widetilde{t}_1$[5] | × | **87**[3] | **-** | **75**[3] |
| $\widetilde{b}_L$ | × | **-** | **-** | **80**[3] |
| $\widetilde{b}_1$[5] | × | **-** | **-** | **71**[6] |

**N.B.** For the sfermion indirect decay, a 100 % BR into neutralino + fermion is assumed.

× The decay channel is not possible

**-** The decay channel is not covered

[1] Valid for any tan$\beta$ and $m_0 > 90$ GeV/$c^2$ and for $-200 < \mu < 200$ GeV/$c^2$ and $0 < M_2 < 400$ GeV
We assumed a neutralino mass greater than 10 GeV/$c^2$.
LEP1 excluded region have been included in this limit.

[2] Obtained for $\mu = -200$ GeV/$c^2$ and tan$\beta = 1.5$.
This result is valid for $\Delta M > 3$ GeV/$c^2$.

[3] Obtained for $\mu = -200$ GeV/$c^2$ and tan$\beta = 1.5$.
This result is valid for $\Delta M > 5$ GeV/$c^2$.

[4] Obtained for $\mu = -200$ GeV/$c^2$ and tan$\beta = 1.5$.
This result is valid for $M_{\widetilde{\chi}^0} > 37$ GeV/$c^2$.

[5] The limit has been derived considering the mixing angle which gives
the maximal decoupling to the Z boson in the squark pair production.

[6] Obtained for $\mu = -200$ GeV/$c^2$ and tan$\beta = 1.5$.
This result is valid for $\Delta M > 20$ GeV/$c^2$.

Table 6: Sparticle mass limits in GeV/$c^2$ from the DELPHI $\not{R}_p$ pair production searches of supersymmetric particles from 1999 and 2000 data.

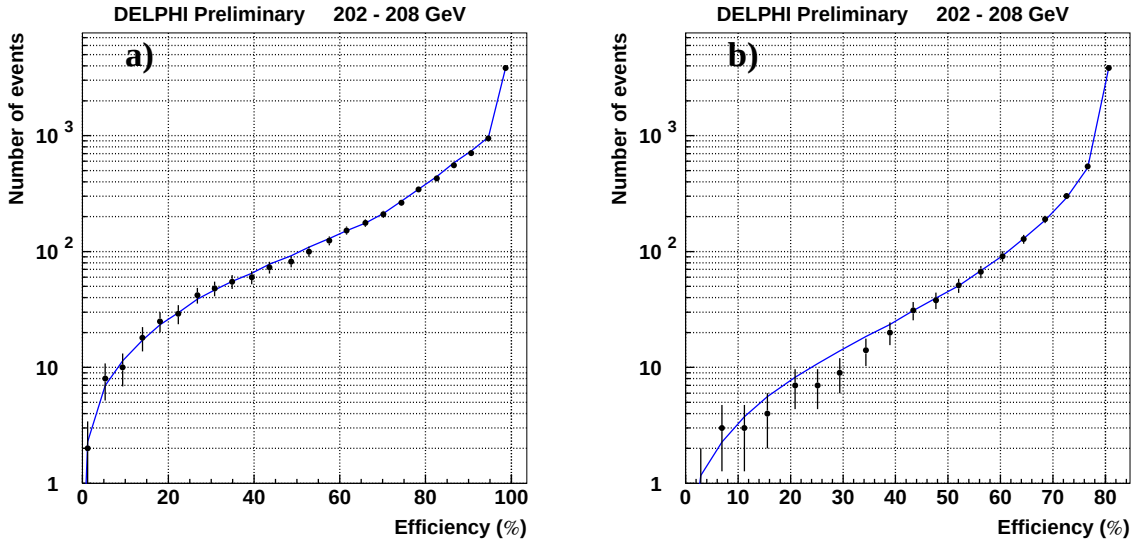


Figure 1: $\bar{\mathrm{U}}\bar{\mathrm{D}}\bar{\mathrm{D}}$: Number of expected events (continuous line) and data events (black dots) versus average signal efficiency for the large neutralino mass search N3 (plot a) and for the large $\Delta$M chargino search C2 (plot b).

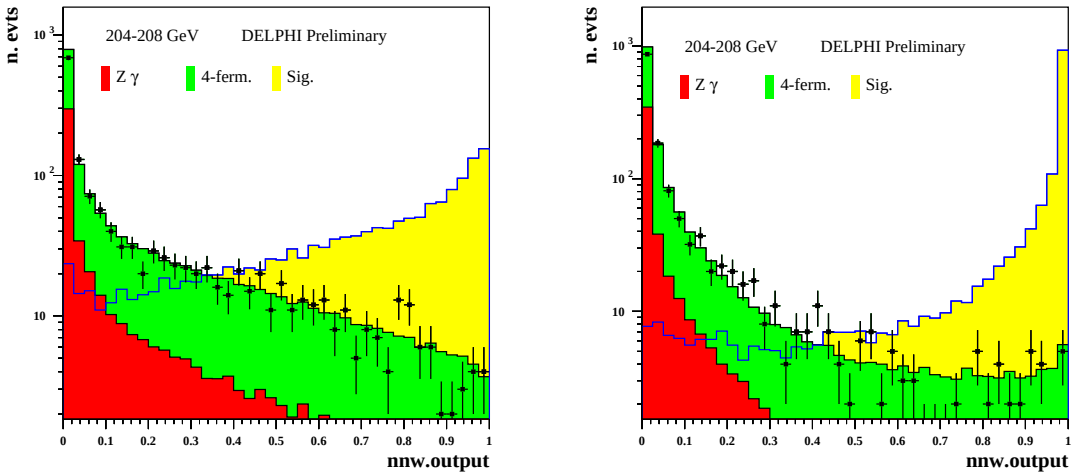


Figure 2: The neural network output distribution of the two window mass analysis for the multi-jets + leptons signal in the $\bar{U}\bar{D}\bar{D}$ selectron analysis. The final signal selection is performed on this distribution.

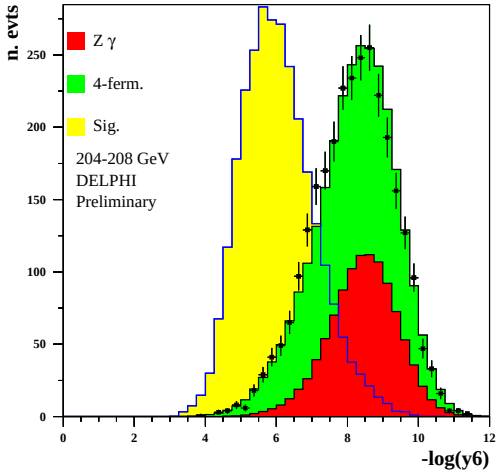


Figure 3: The $y_{65}$ distribution in the $\bar{U}\bar{D}\bar{D}$ smuon analysis.

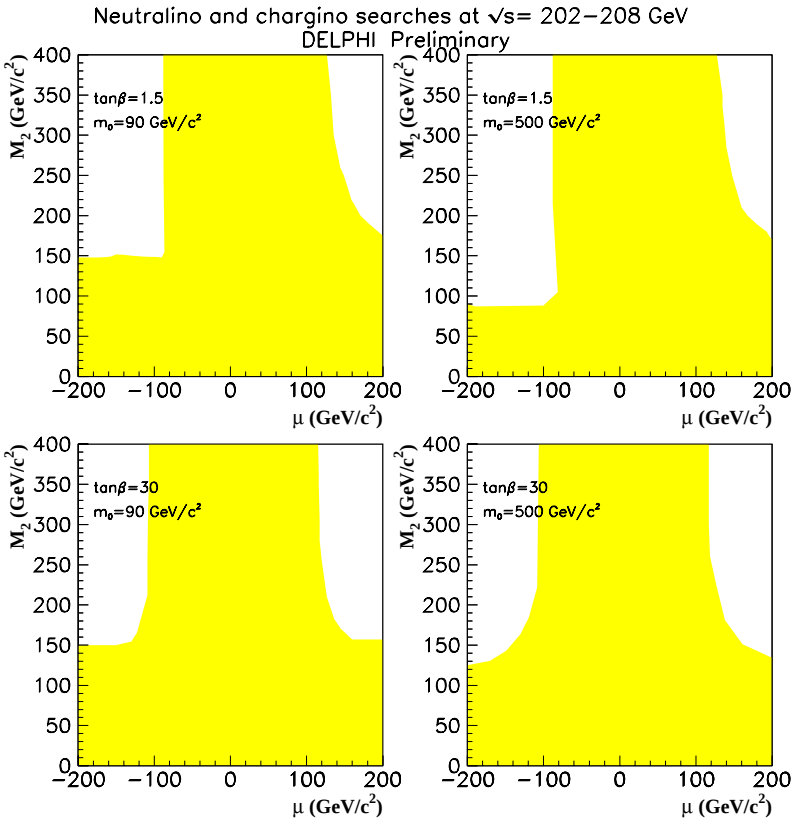


Figure 4: LL$\bar{\text{E}}$: regions in $\mu$, $M_2$ parameter space excluded at 95 % C.L. by the neutralino and chargino searches for two values of tan$\beta$ and two values of $m_0$.

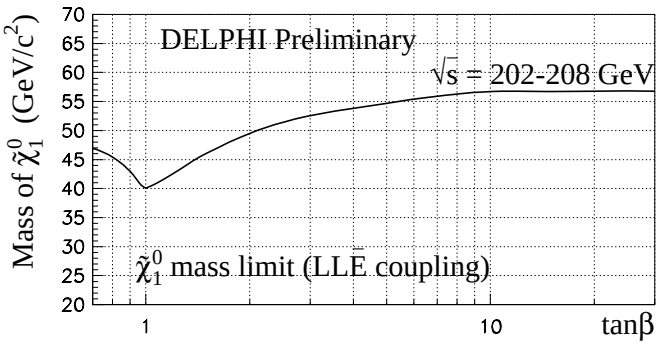


Figure 5: The excluded lightest neutralino mass as a function of tan$\beta$ at 95 % confidence level. This limit is valid for all generation indices $i$,$j$,$k$ of the $\lambda_{ijk}$ coupling and for values of $m_0$ greater than 90 GeV/$c^2$

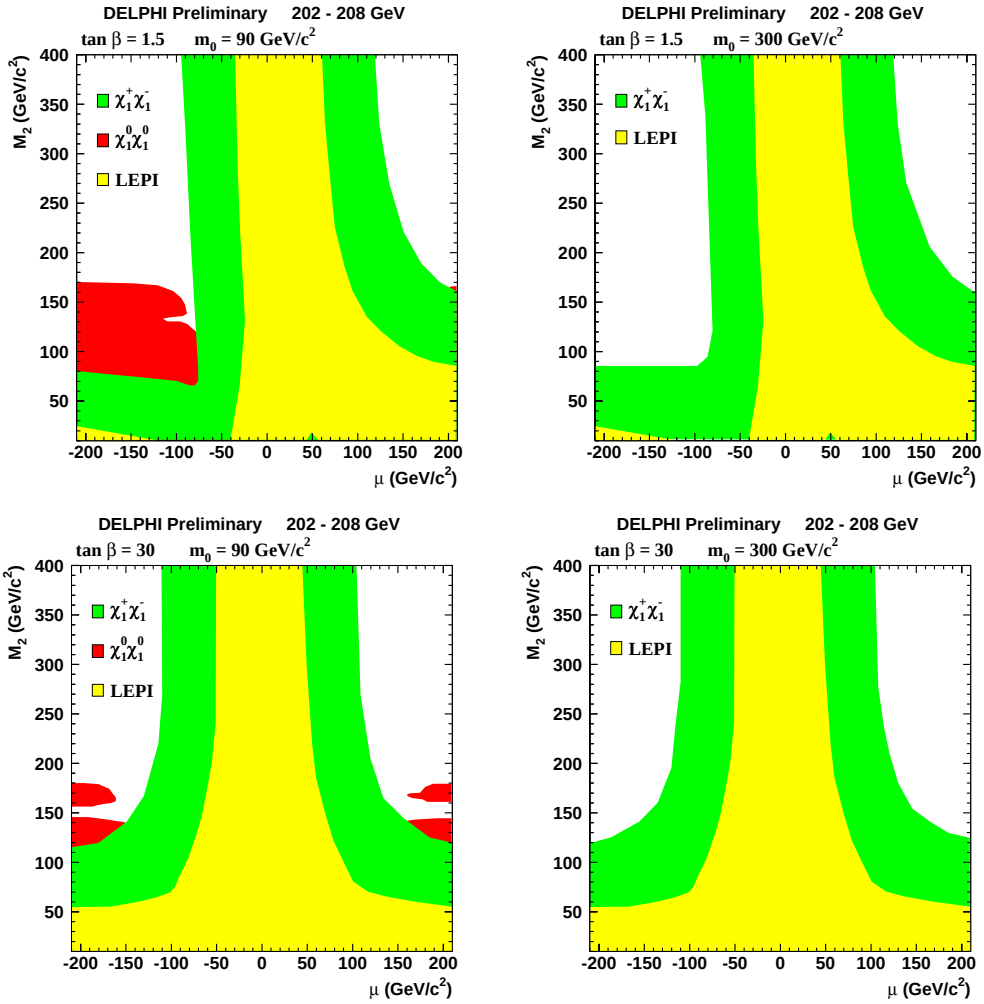


Figure 6: $\bar{\mathrm{U}}\bar{\mathrm{D}}\bar{\mathrm{D}}$ neutralino and chargino searches: exclusion plots in $\mu$, $M_2$ plane. The direct and indirect decay analyses are treated separately for this exclusion.

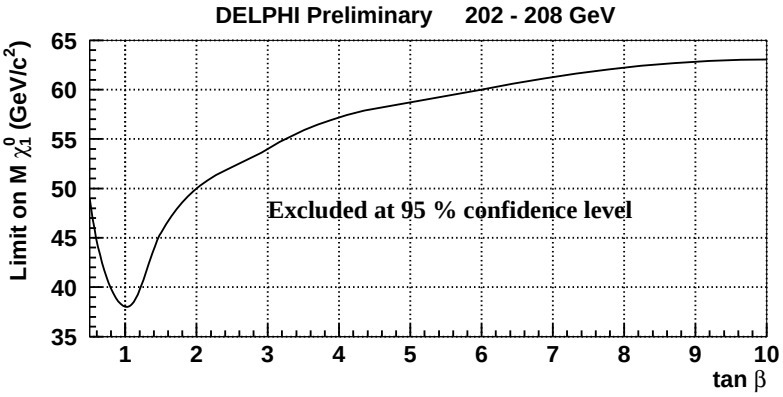


Figure 7: $\bar{\mathrm{U}}\bar{\mathrm{D}}\bar{\mathrm{D}}$: Excluded lightest neutralino mass as a function of tan$\beta$ at 95% confidence level.

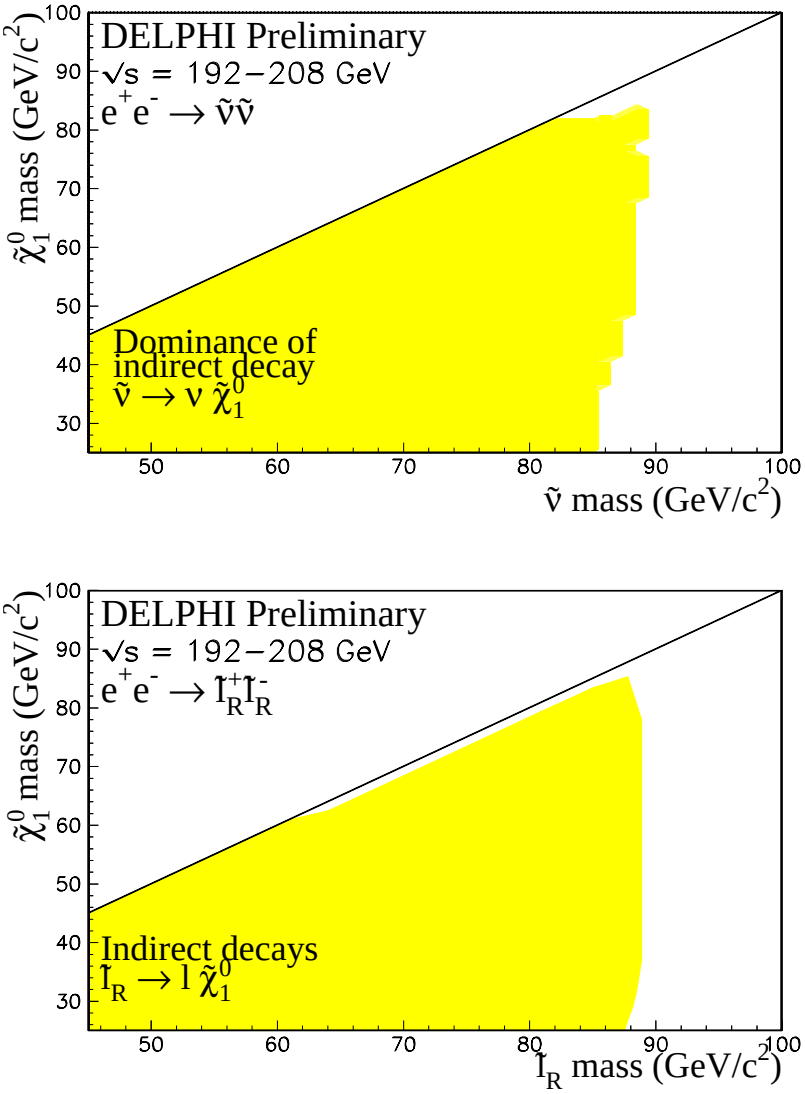


Figure 8: LL$\bar{\text{E}}$: the upper plot shows the excluded region at 95 % C.L. in $m_{\tilde{\nu}}$, $m_{\tilde{\chi}^0}$ plane for $\tilde{\nu}$ pair production for indirect decays. The lower plot shows the excluded region at 95 % C.L. for the charged slepton indirect decay with $\lambda_{133}$ coupling in $m_{\tilde{\ell}_R}$, $m_{\tilde{\chi}^0}$ plane by $\tilde{\ell}_R$ pair production.

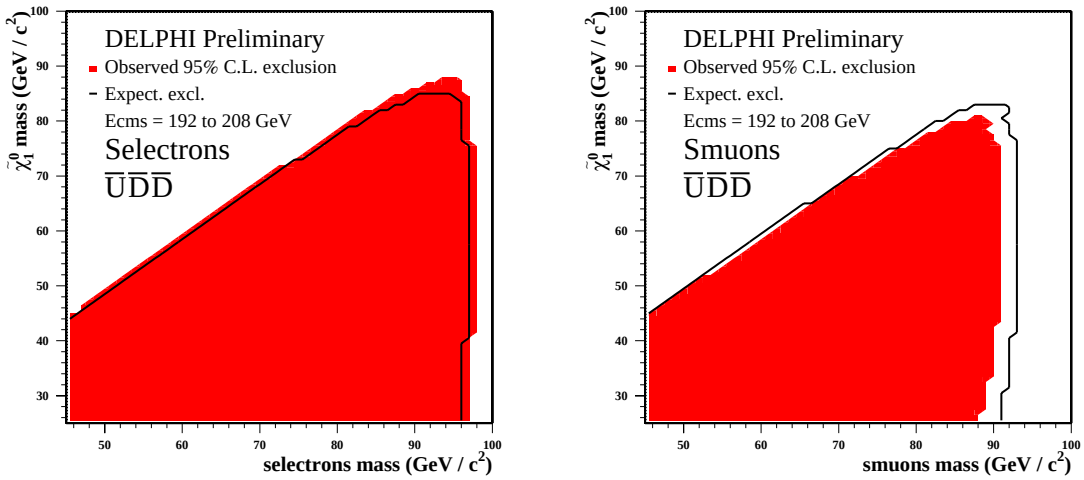


Figure 9: $\bar{\mathrm{U}}\bar{\mathrm{D}}\bar{\mathrm{D}}$: Exclusion domains at 95% confidence level in the $M(\tilde{\chi}_1^0)$, $M(\tilde{e})$ plane for indirect selectron decay in the case of a 100 % branching ratio in the neutralino channel. The superimposed contours illustrate the expected exclusion from the SM background.

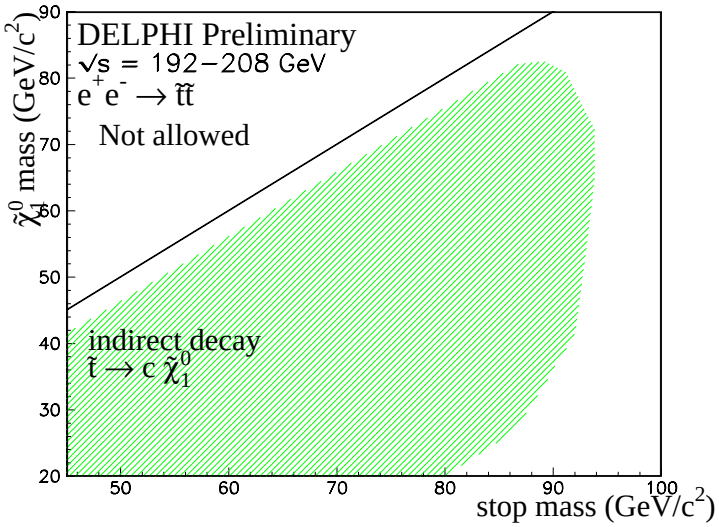


Figure 10: LL$\bar{\text{E}}$: exclusion domain in $m_{\tilde{\chi}^0}$ versus $m_{\tilde{t}}$ for the $\tilde{t}_1$ pair production (with stop indirect decay into $c\tilde{\chi}_1^0$) in case of maximal decoupling to the Z boson.

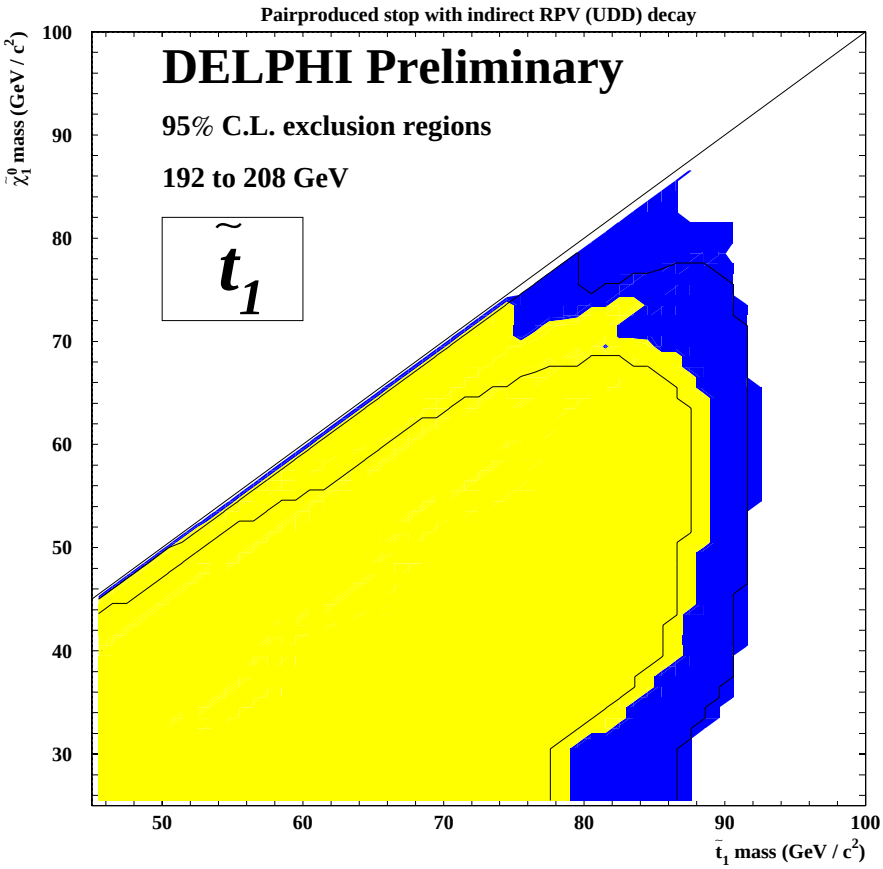


Figure 11: Exclusion domain at 95% confidence level in the $M(\tilde{\chi}_1^0)$, $M(\tilde{t_1})$ plane for indirect stop decays in the case of a 100 % branching ratio in the neutralino channel. The plot shows the exclusion for a stop in the case of no mixing (blue) and with the mixing angle which produces a minimum cross-section (yellow). The diagonal line indicates the degenerate mass limit above which indirect stop decays are forbidden.

# References


[1] P. Fayet, *Phys. Lett.* **B69** (1977) 489;
G. Farrar and P. Fayet, *Phys. Lett.* **B76** (1978) 575.

[2] S. Weinberg, *Phys. Rev.* **D26** (1982) 287.

[3] For reviews, see e.g. H.P. Nilles, *Phys. Rep.***110** (1984) 1; H.E. Haber and G.L. Kane, *Phys. Rep.* **117** (1985) 75.

[4] V. Barger, G.F. Guidice and T. Han, *Phys. Rev.* **D40** (1989) 2987.

[5] R. Barbier et al., *Report of the group on the R–parity violation*, `hep-ph/9810232`.

[6] B.C. Allanach, A. Dedes and H.K. Dreiner, *Phys. Rev.* **D60** (1999) 075014.

[7] P. Abreu et al., *Nucl. Instr. Meth.* **378** (1996) 57.

[8] F.A. Berends, P.H. Daverveldt, R. Kleiss, *Computer Phys. Comm.* **40** (1986) 271,285 and 309.

[9] S. Nova, A. Olshevski, T. Todorov, DELPHI note 90-53(1990).

[10] S. Jadach, W. Placzek, B.F.L. Ward, *Phys. Lett.* **B390** (1997) 298.

[11] S. Jadach, Z. Was, *Computer Phys. Comm.* **79** (1994) 503.

[12] T. Sjostrand, *Computer Phys. Comm.* **82** (1994) 74.

[13] F.A. Berends, R. Kleiss, R. Pittau, *Computer Phys. Comm.* **85** (1995) 437.

[14] J. Fujimoto *et al.*, *Computer Phys. Comm.* **100** (1997) 128.

[15] S. Katsanevas, P. Morawitz, *Computer Phys. Comm.* **112** (1998) 227
.N. Ghodbane hep-ph/9909499.

[16] C. Berat, E Merle, DELPHI 2000-015 CONF 336.

[17] R. Barbier, N. Benekos, C. Berat, P. Jonsson, F. Ledroit-Guillon, R. López-Fernández, E. Merle, Th. Papadopoulou, V. Poireau, DELPHI 2000-084 CONF 383.
Delphi Collaboration, *Phys. Lett.* **B487** (2000) 36..
Delphi Collaboration, *Phys. Lett.* **B500** (2001) 22..

[18] S. Catani et al., *Phys. Lett.* **B269** (1991) 432.

[19] S. Bentvelsen and I. Meyer, Eur. Phys. J. C4 (1998) 623.

[20] Yu.L. Dokshitzer, G.D. Leder, S. Moretti, B.R. Webber, J. High Energy Phys. 08 (1997) 001.

[21] A. Zell et al., SNNS User manual, Version 4.1, Report N 6/95.

[22] MLPfit, written by J.Schwindling, B.Mansoulié and O.Couet. For futher information, see http://home.cern.ch/˜schwind/MLPfit.html.

[23] G. C. Fox, S. Wolfram, *Nucl. Phys.* **B149** (1979) 413..G. C. Fox, S. Wolfram, *Phys. Lett.* **B82** (1979) 134.

[24] R.M. Barnett et al., *Phys. Rev.* **D54** (1996) 1.

[25] Particle Data Group, Phys. Rev. D54 (1996) 1.

[26] A. Read DELPHI 97-158 PHYS 737.